

# Density Functional Theory Calculations of Vibrational Circular Dichroism in Transition Metal Complexes: Identification of Solution Conformations and Mode of Chloride Ion Association for (+)-Tris(ethylenediaminato)cobalt(III)<sup>†</sup>

Teresa B. Freedman,\* Xiaolin Cao, Daryl A. Young,<sup>‡</sup> and Laurence A. Nafie\*

Department of Chemistry, Syracuse University, Syracuse, New York 13244-4100

Received: August 7, 2001; In Final Form: January 7, 2002

Density functional theory calculations of the vibrational circular dichroism (VCD) spectra of a transition metal complex, (+)-tris(ethylenediaminato)cobalt(III) as a free ion and with associated chloride ions, are reported. By comparison with experimental data obtained in our laboratory in 1986 (Young et al. *J. Am. Chem. Soc.* **1986**, *108*, 7255) and new measurements, this study identifies, for the first time, the geometry and absolute configuration of the association complex as  $\Lambda$ - $\delta\delta\delta$ -Co(en)<sub>3</sub>Cl<sub>2</sub><sup>+</sup>, in which two chloride ions each associate with three NH bonds along the C<sub>3</sub>-axis of a D<sub>3</sub>-symmetry complex. The DFT calculations, carried out with both the LanL2DZ and 6-31G(d)[C, H, N]/Stuttgart ECP [Co] basis sets, predict the energy order of ethylenediamine ring conformations as  $\lambda\lambda\lambda < \lambda\lambda\delta < \lambda\delta\delta < \delta\delta\delta$  for the free (gas phase)  $\Lambda$ -Co(en)<sub>3</sub><sup>3+</sup> ion, an order opposite to that deduced from solution studies. The VCD studies identify the  $\delta$ -conformation as the most prevalent in solution for halide and sulfate counterions, suggesting an interaction with solvent or weakly associated counterions that stabilizes this conformation.

## Introduction

Vibrational circular dichroism, the differential absorbance of left and right circularly polarized infrared radiation by a chiral molecule during vibrational excitation, is a probe of absolute configuration and solution conformation.<sup>1–3</sup> Recent incorporation of routines into Gaussian 98<sup>4</sup> for the calculation of VCD intensities<sup>5</sup> has greatly expanded these applications. Excellent agreement between experimental and calculated VCD spectra<sup>1,3,6</sup> is now routinely found for calculations on organic molecules of moderate size, carried out at the DFT level with gauge-invariant atomic orbitals, most often with B3LYP or BPW91 functionals and a 6-31G(d) basis set.<sup>6,7</sup> Although comparisons of experimental and calculated VCD spectra have focused primarily on the mid-infrared region from 1800 to 800 cm<sup>-1</sup>, agreement between experimental and ab initio and DFT calculations has also been demonstrated for hydrogen stretching motions.<sup>8,9</sup> However, to date only one calculation of the VCD for a metal complex has been reported in the literature.<sup>10</sup> We have recently begun application of VCD intensity calculations to metal complexes with open and closed shell configurations, including a recent application to metal complexes with sparteine.<sup>10</sup>

To test the agreement between observed and calculated VCD for a closed shell transition metal complex that can assume a variety of conformations, we have calculated the VCD spectra for (+)-tris(ethylenediaminato)cobalt(III) (Co(en)<sub>3</sub><sup>3+</sup>), with and without associated chloride ions. This complex cation is a benchmark for studying optical activity in metal complexes, serving as the subject of the first absolute configuration determination with anomalous X-ray scattering,<sup>11</sup> the first solution and solid-state electronic circular dichroism measurements of the same transition metal complex,<sup>12</sup> recent extension of CD measurement to the X-ray region,<sup>13</sup> one of the first VCD

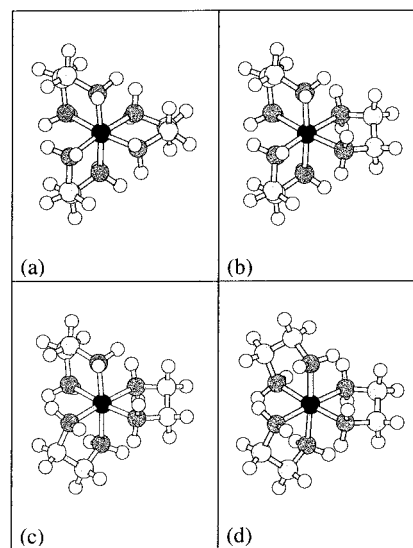


**Figure 1.**  $\Lambda$ -Co(en)<sub>3</sub><sup>3+</sup> conformations, viewed along the C<sub>3</sub>-axis: (a)  $\delta\delta\delta$ , (b)  $\delta\delta\lambda$ , (c)  $\delta\lambda\lambda$ , and (d)  $\lambda\lambda\lambda$ .

studies on metal complexes,<sup>14</sup> and an ab initio calculation of chiroptical spectra in the visible region.<sup>15</sup> Our VCD measurements of this system in 1986<sup>16</sup> suggested that the chloride ion association stabilizes a specific conformation of the en rings in the presence of excess chloride.<sup>14</sup>

The achiral ethylenediamine ligand can assume two enantiomeric conformations, with the C–C bond nearly parallel ( $\delta$ -form) or oblique ( $\lambda$ -form) to the C<sub>3</sub>-axis in the  $\Lambda$ -configuration, leading to four conformations for the complex (Figure 1). On the basis of an assessment of nonbonded interactions, the  $\delta\delta\delta$  form for the  $\Lambda$ -Co(en)<sub>3</sub><sup>3+</sup> configuration was suggested to be the most favored energetically,<sup>17</sup> but the intermediate  $\lambda\delta\delta$  and  $\lambda\lambda\delta$  are statistically favored over the extreme forms.<sup>18</sup> NMR studies<sup>19</sup> indicate that 60–70% of the en rings are  $\delta$  for

<sup>†</sup> Part of the special issue "Mitsuo Tasumi Festschrift".

<sup>‡</sup> Current Affiliation: Celanese, Ltd, Corpus Christi, TX.

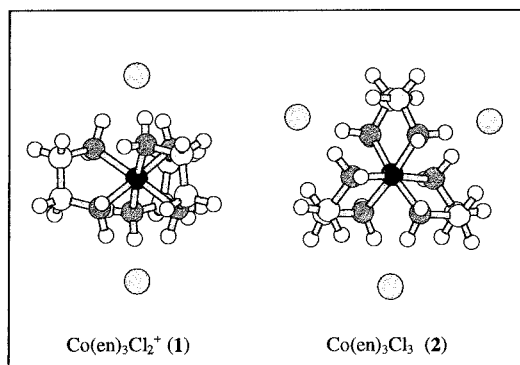


**Figure 2.** Geometries of  $\Lambda$ - $\delta\delta\delta$ - $\text{Co(en)}_3^{3+}$  with two associated chloride ions along the  $C_3$ -axis ( $\text{Co(en)}_3\text{Cl}_2^+$ ) and three associated chloride ions along the three  $C_2$ -axes ( $\text{Co(en)}_3\text{Cl}_3$ ).

complexes with a  $\Lambda$ -configuration. From their effect on NMR<sup>19</sup> and electronic CD spectra,<sup>20,21</sup> counterions have been deduced to influence the en ring conformation in tris-chelated Co(III) complexes in solution. However, the specific nature of this interaction cannot be determined from those measurements. By contrast, VCD uniquely combines stereostructural specificity with subpicosecond time-domain response. As a result, we find that VCD provides a direct probe of the solution conformation of this complex through the affect of the ion association on the ligand vibrations and the VCD intensities.

Association of a chloride ion with NH bonds from adjacent en rings stabilizes the  $\delta$ -conformation for the  $\Lambda$ -configuration. We consider here two possible complexes of  $\Lambda$ - $\text{Co(en)}_3^{3+}$  with all three en rings in the  $\delta$  conformation, one with three chloride ions associated with NH bonds along the three  $C_2$ -axes, and a second with two chloride ions associated with NH bonds along the  $C_3$ -axis of this  $D_3$ -symmetry complex (Figure 2).

### Experimental and Computational Methods

The preparation of the iodide and chloride salts of (+)- $\text{Co(en)}_3^{3+}$  and the details of the VCD measurements are reported in our 1986 publication.<sup>14</sup> The (+)-enantiomer is assigned to the  $\Lambda$ -configuration. The absorption and VCD spectra presented in the earlier study were recorded with a dispersive instrument in the NH- and CH-stretching regions,<sup>22</sup> and with a modified Nicolet 7199 FT-VCD instrument in the 1600–1100  $\text{cm}^{-1}$  region.<sup>23</sup> For comparison to the calculations, selected spectra from this previous study are reproduced here, with relevant experimental conditions included in the corresponding figure caption. For improved signal-to-noise and spectral coverage in the 1600–1100  $\text{cm}^{-1}$  region, new VCD spectra were recorded for a sample of  $\text{Co(en)}_3\text{I}_3$  from our original study, in  $\text{DMSO-}d_6$  with a 10-fold excess of LiCl, utilizing a modified Chiralir VCD spectrometer (ABB Bomem/BioTools).<sup>24</sup>

The optimized geometries and IR and VCD spectra for the four  $\Lambda$ - $\text{Co(en)}_3^{3+}$  conformers shown in Figure 1 and the association complexes **1** and **2** shown in Figure 2 were calculated with Gaussian 98, utilizing a B3LYP functional and the basis set LanL2DZ in Gaussian 98, which includes Dunning/Huzinaga full double- $\zeta$  on the first row elements, and the Los Alamos ECP (effective core potential) plus double- $\zeta$  on Na–Bi.<sup>25,26</sup> The optimized geometries of the association complexes corresponding to **1** with a single chloride ion and corresponding to **2** with one or two chloride ions were also calculated with this basis set. The VCD intensities were calculated with the magnetic field perturbation method<sup>27</sup> incorporated into Gaussian 98, using gauge invariant atomic orbitals.<sup>5,7</sup> For the conformers in Figure 1, these calculations were also carried out with the

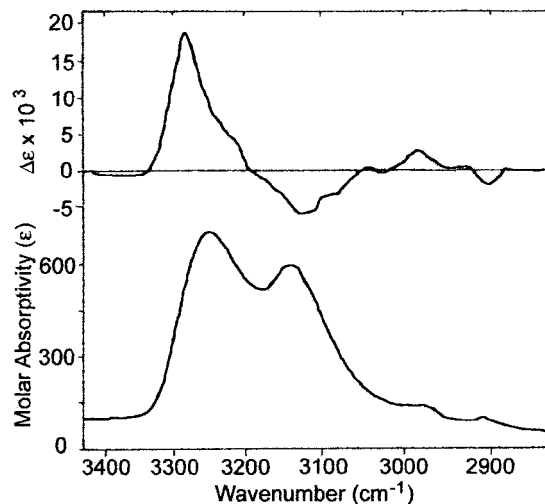


**Figure 3.** NH- and CH-stretching absorbance (lower) and VCD spectra (upper) of  $\Lambda$ - $[\text{Co(en)}_3]\text{I}_3$ , 0.07 M in 1 M  $\text{D}_2\text{SO}_4$ , 50  $\mu\text{m}$  path length cell with Infracil windows, 12  $\text{cm}^{-1}$  resolution.

6-31G(d) basis set on C, N, and H and the Stuttgart relativistic small core, ECP basis set for cobalt.<sup>28</sup> For comparison among calculated spectra of the four conformers of the isolated ion, the calculated frequencies were uniformly scaled by 0.97 and calculated intensities were converted to Lorentzian bands with 5- $\text{cm}^{-1}$  half-width and plotted with Axum (Mathsoft, Inc.). For more direct comparison to experiment in the case of chloride association, the calculated intensities were converted to Lorentzian bands with 30  $\text{cm}^{-1}$  half-width for the associated NH-stretching modes, 15  $\text{cm}^{-1}$  for free NH- and CH-stretches, and 6  $\text{cm}^{-1}$  for the region below 2000  $\text{cm}^{-1}$ , as estimated from the observed spectra. For the association complexes, the frequencies of the free NH-stretches and the CH-stretches were uniformly scaled by 0.94 to align the frequencies of the calculated CH-stretches with the observed. The frequencies of the calculated associated NH bonds were uniformly scaled by 1.03 for comparison with the observed data, since the shift to lower frequency due to ion association is overestimated in the calculation, which is for the gas-phase species. Descriptions of calculated modes discussed below are based on animations of the modes with Gaussview (Gaussian, Inc.) or HyperChem (Hypercube, Inc.).

### Results

The observed absorption and VCD spectra of  $\Lambda$ - $\text{Co(en)}_3\text{I}_3$  in the presence of excess sulfate ion<sup>14</sup> is reproduced in Figure 3 for the NH- and CH-stretching regions. The CH-stretching spectra for samples in  $\text{D}_2\text{O}$  as a function of halide ion<sup>14</sup> are shown in Figure 4. The absorption and VCD spectra of  $\Lambda$ - $\text{Co(en)}_3^{3+}$  for a sample of the chloride salt in  $\text{DMSO-}d_6$  with a 10-fold excess of chloride<sup>14</sup> are displayed in Figure 5 for the NH/CH-stretching regions, compared to the calculation for **1**. Our new measurements of  $\Lambda$ - $\text{Co(en)}_3\text{I}_3$  in  $\text{DMSO-}d_6$  with a 10-fold excess of LiCl are compared to the calculated spectra of **1** and **2** in the 1600–1130  $\text{cm}^{-1}$  region in Figure 6. The calculated spectra shown in Figures 5 and 6 utilized the B3LYP functional and LanL2DZ basis set.

The relative energies (kcal/mol) calculated for the  $\Lambda$ - $\text{Co(en)}_3^{3+}$  isolated (gas phase) ion in the  $\delta\delta\delta$ ,  $\delta\delta\lambda$ ,  $\delta\lambda\lambda$ , and  $\lambda\lambda\lambda$  conformations are +1.0, +0.30, +0.03, and 0.0, respectively, for the LanL2DZ basis set, and +0.81, +0.24, +0.04, and 0.0, respectively, for the 6-31G(d)[C, H, N]/Stuttgart [Co] basis set. The calculated spectra for the two basis sets are similar, with

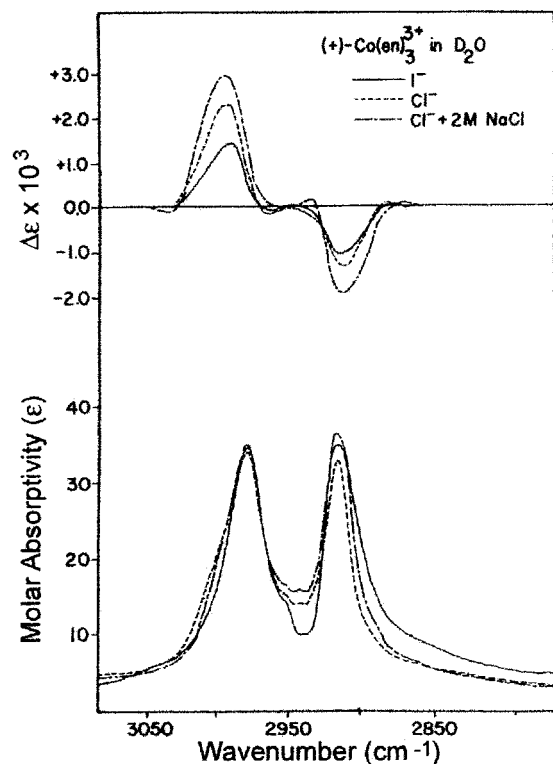


**Figure 4.** CH-stretching absorbance (lower) and VCD spectra (upper) of  $\Lambda$ -[Co(en)<sub>3</sub>]<sup>3+</sup>, 0.10 M in D<sub>2</sub>O, 200- $\mu$ m path length CaF<sub>2</sub> cell: (—) iodide salt, (---) chloride salt, (- · -) chloride salt with 2M NaCl.

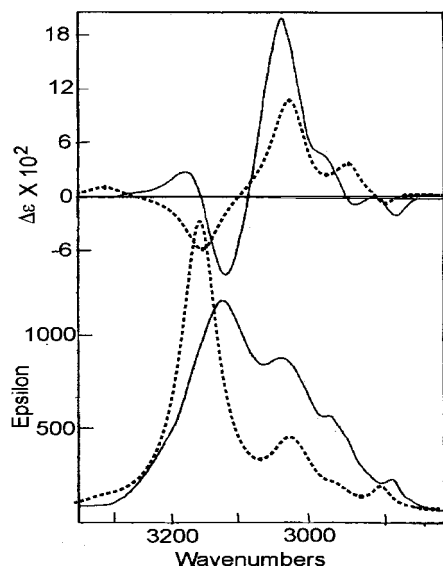


**Figure 5.** NH/CH-stretching absorbance (lower) and VCD (upper) spectra of  $\Lambda$ -[Co(en)<sub>3</sub>]<sup>3+</sup>, 0.060 M with 0.6 M LiCl in DMSO-*d*<sub>6</sub> in 100- $\mu$ m path length CaF<sub>2</sub> cell, 12 cm<sup>-1</sup> resolution (solid line), compared to calculated spectra (dashed line) for Co(en)<sub>3</sub>Cl<sub>2</sub><sup>+</sup> (1), DFT (B3LYP/LanL2DZ).

some variation in relative intensities. The free energies (kcal/mol) calculated with the LanL2DZ basis set for changes in ring conformation, including the statistical entropy term for the  $\delta\delta\lambda$  and  $\delta\lambda\lambda$  forms ( $-RT \ln 3$ ), are  $-0.93$  ( $\delta\delta\delta \rightarrow \delta\delta\lambda$ ),  $-1.17$  ( $\delta\delta\delta \rightarrow \delta\lambda\lambda$ ) and  $-0.64$  ( $\delta\delta\delta \rightarrow \lambda\lambda\lambda$ ).

Since agreement with the experimental intensity patterns was somewhat better for calculations with the LanL2DZ basis set, only those results are displayed here. The calculated absorbance and VCD spectra for the four  $\Lambda$ -Co(en)<sup>3+</sup> conformers are presented in Figure 7 (NH-stretches), Figure 8 (CH-stretches)

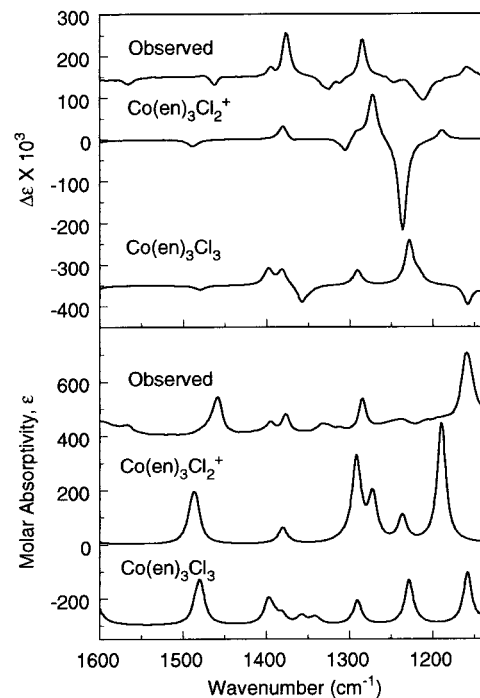


**Figure 6.** Mid-IR absorption (lower) and VCD (upper) spectra of  $\Lambda$ -[Co(en)<sub>3</sub>]<sup>3+</sup> in DMSO-*d*<sub>6</sub>, iodide salt, 0.060 M with 0.6 M LiCl (193- $\mu$ m path length BaF<sub>2</sub> cell, 4-cm<sup>-1</sup> resolution, 10-h collection, solvent baseline corrected), compared to calculated spectra for Co(en)<sub>3</sub>Cl<sub>2</sub><sup>+</sup> (1) and Co(en)<sub>3</sub>Cl<sub>3</sub> (2), DFT (B3LYP/LanL2DZ), 6-cm<sup>-1</sup> half-width Lorentzian bands, frequencies scaled by 0.97. Spectra offset for clarity.

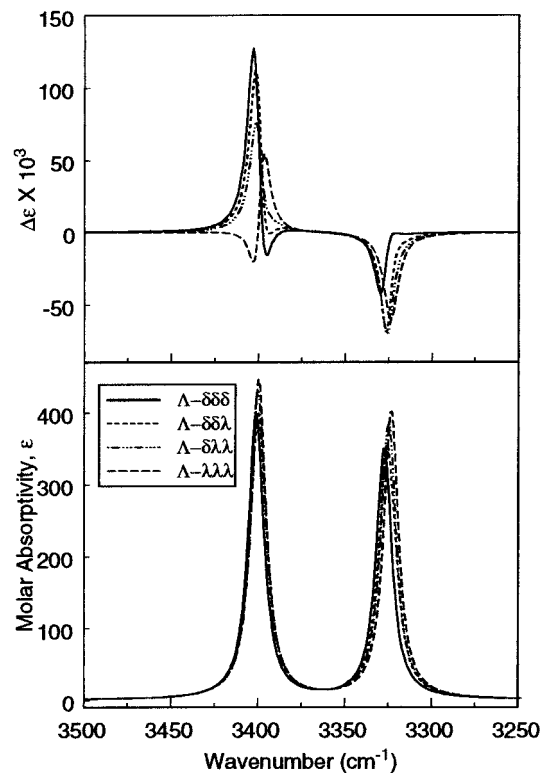


**Figure 7.** Calculated NH-stretching absorbance and VCD spectra for  $\Lambda$ -[Co(en)<sub>3</sub>]<sup>3+</sup> conformers, DFT (B3LYP/LanL2DZ), scale factor 0.97, 5-cm<sup>-1</sup> half-width Lorentzian bands.

and Figure 9 (mid-IR region). Calculated NH/CH-stretching VCD spectra for association complexes 1 and 2 are compared in Figure 10. Calculated NH-stretching frequencies, intensities, and band assignments for 1 and 2 are listed in Table 1, where

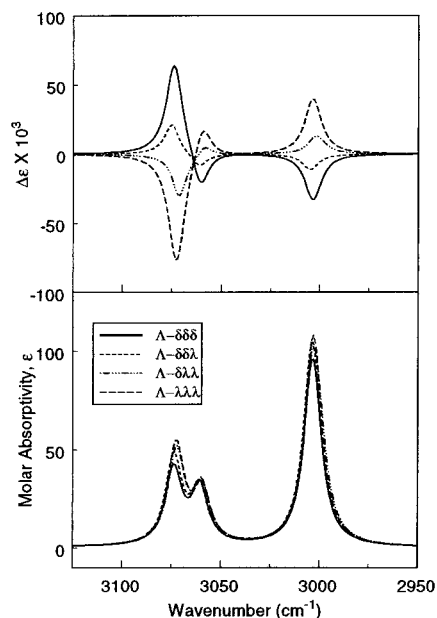


**Figure 8.** Calculated CH-stretching absorbance and VCD spectra for  $\Lambda$ -[Co(en) $_3$ ] $^{3+}$  conformers, DFT (B3LYP/LanL2DZ), scale factor 0.97, 5-cm $^{-1}$  half-width Lorentzian bands.

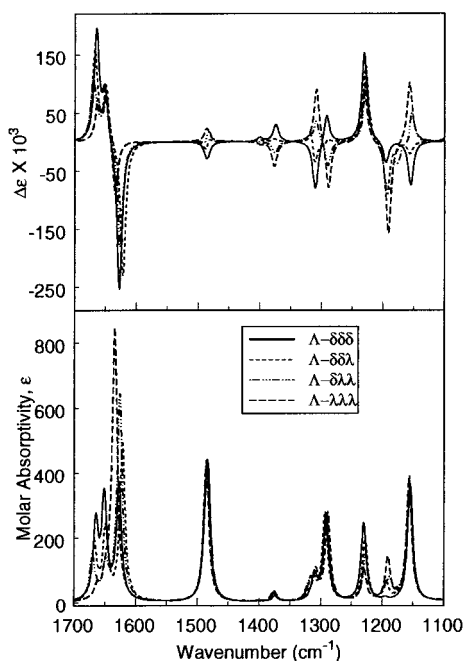


**Figure 9.** Calculated mid-IR absorbance and VCD spectra for  $\Lambda$ -[Co(en) $_3$ ] $^{3+}$  conformers, DFT (B3LYP/LanL2DZ), scale factor 0.97, 5-cm $^{-1}$  half-width Lorentzian bands.

the calculated intensities represent a sum of the dipole or rotational strengths for the bands in each region. With a single chloride ion lying along the  $C_3$ -axis, an intense ( $-/+$ ) VCD pattern for the associated NH-stretches is calculated, similar to that for two chloride ions in **1**, and an intense ( $+/-$ ) VCD pattern is calculated for the associated NH-stretches for the complexes with one or two chloride ions lying along  $C_2$ -axes, similar to the pattern for three chloride ions in **2**. The observed frequencies and intensities at band maxima for  $\Lambda$ -Co(en) $_3$  $^{3+}$  in DMSO- $d_6$  with excess chloride ion, from our original study<sup>16</sup> and new measurements, are compared to those obtained from the calculations on  $\Lambda$ -Co(en) $_3$ Cl $_2^+$  in the  $\delta\delta\delta$ -conformation in Table 2.

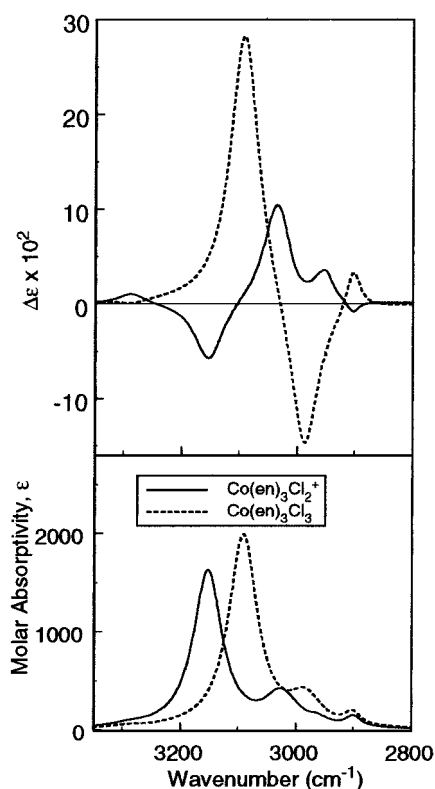


**Figure 10.** Calculated NH/CH-stretching molar absorptivity (lower traces) and VCD spectra (upper traces) for  $\Lambda$ - $\delta\delta\delta$ -Co(en) $_3$  $^{3+}$  with two associated chloride ions (Co(en) $_3$ Cl $_2^+$ , **1**) and three associated chloride ions (Co(en) $_3$ Cl $_3$ , **2**). Lorentzian bands with 30-cm $^{-1}$  half-width for associated NH-stretches, 15-cm $^{-1}$  half-width for free NH- and CH-stretches.

**TABLE 1: Calculated NH-stretching Frequencies, Intensities, and Mode Assignments for **1** and **2****

frequency (scaled, cm $^{-1}$ )	dipole strength	rotational strength	stretching mode assignment
Co(en) $_3$ Cl $_2^+$ ( <b>1</b> )			
3290	65	+77	free NH (A $_1$ , A $_2$ , 2E)
3165	0	0	NH $\cdots$ Cl (A $_1$ )
3153	4500	-445	NH $\cdots$ Cl (A $_2$ )
3023	1047	+698	NH $\cdots$ Cl (2E)
2958	93	+121	CH $_2^a$ (A $_1$ , A $_2$ , 2E)
2901	162	-43	CH $_2^s$ (A $_1$ , A $_2$ , 2E)
Co(en) $_3$ Cl $_3$ ( <b>2</b> )			
3290	41	-30	free NH (A $_1$ , A $_2$ , 2E)
3107	0	0	NH $\cdots$ Cl (A $_1$ )
3091	5515	+2067	NH $\cdots$ Cl (E)
2985	821	-1274	NH $\cdots$ Cl (A $_2$ , E)
2967	36	+33	CH $_2^a$ (A $_1$ , A $_2$ , 2E)
2901	187	+167	CH $_2^s$ (A $_1$ , A $_2$ , 2E)

<sup>a</sup> 10 $^{-40}$  esu $^2$  cm $^2$ . <sup>b</sup> 10 $^{-44}$  esu $^2$  cm $^2$ . <sup>c</sup> CH $_2^a$  = antisymmetric CH $_2$ -stretch. <sup>d</sup> CH $_2^s$  = symmetric CH $_2$ -stretch.

## Discussion

For a complex with  $D_3$  symmetry, the A $_1$  modes are inactive, and the IR-active A $_2$ /E mode pairs will generate bisignate VCD features when these two components are resolved. For Co(en) $_3$  $^{3+}$ , the modes involving predominantly NH motion should be most sensitive to configuration, whereas CH-modes should be most sensitive to the ring conformation. The calculated spectra for the four conformations agree with this predicted pattern. The antisymmetric NH $_2$ -stretches (Figure 7, scaled frequency  $\sim$ 3400 cm $^{-1}$ ) generate a positively biased VCD couplet for the  $\delta\delta\delta$  ( $+/-$ ) and  $\lambda\lambda\lambda$  ( $-/+$ )  $D_3$ -symmetry cases; the VCD is predominantly positive for all four conformations.



**TABLE 2: Comparison of Observed Absorbance and VCD Spectra of  $\text{Co}(\text{en})_3^{3+}$  with Excess Chloride Ion with Calculated Spectra for  $\Lambda$ - $\delta\delta\delta$ - $\text{Co}(\text{en})_3\text{Cl}_2^+$  (**1**)**

observed <sup>a</sup>			$\text{Co}(\text{en})_3\text{Cl}_2^+$ , calculated <sup>b</sup>			assignment <sup>c</sup>
frequency <sup>d</sup>	$\epsilon_{\text{max}}^e$	$10^3\Delta\epsilon_{\text{max}}$	frequency	$\epsilon_{\text{max}}$	$10^3\Delta\epsilon_{\text{max}}$	
3180		+28	3288	105	+10	Free $\text{NH}_2^g$ str.
3125	1098	-89	3153	1630	-60	$\text{NH}\cdot\text{Cl}$ str. ( $A_2$ )
3041	792	+200	3035	415	+104	$\text{NH}\cdot\text{Cl}$ str. (E)
2975	125	+43	2955	152 (sh)	+36	$\text{CH}_2^g$ stretch
2950	120	-8				$\text{CH}_2^s$ stretch
2893	80	-23	2903	153	-8	$\text{CH}_2^s$ stretch
			1629	172	-161	$\text{NH}_2$ scissors
1458, 1462	144	-17	1487	196	-16	$\text{CH}_2$ scissors
1394	54	+25				$\text{CH}_2$ wag
1377	81	+107	1380	62	+31	$\text{CH}_2$ wag ( $A_2$ )
1331, 1325	45	-29	1306	(sh)	-27	$\text{CH}_2$ twist, $\text{NH}_2$ wag ( $A_2$ )
			1292	330	+22	$\text{CH}_2$ twist, $\text{NH}_2$ wag (E)
1284	136	+90	1273	204	+106	$\text{NH}_2$ twist, $\text{CH}_2$ rock
1236, 1247	60	-13				$\text{NH}_2$ wag
1211	60 (sh)	-56	1237	112	-217	$\text{NH}_2$ wag
1160	306	+23	1190	447	+20	$\text{NH}_2$ wag, $\text{CH}_2$ twist

<sup>a</sup> Hydrogen stretching data from ref 13, 0.060 M in  $\text{DMSO}-d_6$  with 0.6 M  $\text{LiCl}$ . <sup>b</sup> Lorentzian bands. Below 2000  $\text{cm}^{-1}$ : 6- $\text{cm}^{-1}$  half-width, frequencies scaled by 0.97. Free  $\text{NH}/\text{CH}$ -stretch: 15- $\text{cm}^{-1}$  half-width, frequencies scaled by 0.94. Associated  $\text{NH}$ -stretch: 30- $\text{cm}^{-1}$  half-width, frequencies scaled by 1.03. <sup>c</sup>  $\text{NH}_2^g$ ,  $\text{CH}_2^g$ : antisymmetric stretch.  $\text{CH}_2^s$ : symmetric stretch. <sup>d</sup>  $\text{cm}^{-1}$ ; frequency for absorbance followed by frequency for VCD, when these differ by more than 5  $\text{cm}^{-1}$ . <sup>e</sup>  $\epsilon$ , molar absorptivity in  $10^3 \text{ cm}^2 \text{ mol}^{-1}$ .

The symmetric  $\text{NH}_2$ -stretching VCD ( $\sim 3325 \text{ cm}^{-1}$ ) has net negative intensity for the  $\Lambda$ -configuration, independent of ring conformation. Comparison of the calculations in this region with the experimental spectrum for (+)- $\text{Co}(\text{en})_3^{3+}$  in Figure 3 shows agreement in sign for the antisymmetric and symmetric  $\text{NH}$ -stretching VCD for the  $\Lambda$ -configuration. This comparison provides an independent identification of the absolute configuration of the sample.

The calculated  $\text{CH}$ -stretching VCD spectra (Figure 8) exhibit strong sensitivity to ring conformation, with net positive VCD for the antisymmetric  $\text{CH}_2$ -stretches ( $\sim 3074, 3060 \text{ cm}^{-1}$ ) and net negative VCD for the symmetric  $\text{CH}_2$ -stretches ( $\sim 3004 \text{ cm}^{-1}$ ) for the  $\delta$ -conformation of the en ring, and the opposite signs for these regions for the  $\lambda$ -conformation. Comparison with the observed VCD (Figures 3 and 4) provides identification of the dominant ring conformation as  $\delta$  for the  $\Lambda$ -configuration aqueous solution of  $\text{Co}(\text{en})_3^{3+}$  salts and demonstrates that addition of excess chloride ion increases the fraction of rings in the  $\delta$ -conformation.

In the 1700–1100  $\text{cm}^{-1}$  region, the calculated VCD for modes dominated by  $\text{NH}_2$  scissors motion ( $\sim 1665 \text{ cm}^{-1}$ , E; 1650  $\text{cm}^{-1}$ ,  $A_2$ ) or  $\text{NH}_2$  wagging motion ( $\sim 1230 \text{ cm}^{-1}$ ,  $A_2$ ; 1190  $\text{cm}^{-1}$ , E) are markers for configuration, whereas the VCD sign for modes involving predominantly  $\text{CH}_2$ -scissors ( $\sim 1485 \text{ cm}^{-1}$ ),  $\text{CH}_2$ -wag ( $\sim 1375 \text{ cm}^{-1}$ ), or  $\text{CH}_2$ -twist ( $\sim 1310, 1290 \text{ cm}^{-1}$ ) correlates with the ring conformation. The calculated VCD for the  $\Lambda$ - $\delta\delta\delta$  structure (Figure 9) correlates well with the observed VCD for  $\Lambda$ - $\text{Co}(\text{en})_3^{3+}$  in  $\text{DMSO}-d_6$  in the presence of excess chloride ion (Figure 6, Table 2), taking into account shifts to higher energy for the associated  $\text{NH}_2$  wagging modes. Comparison of the calculations shown in Figure 9 with our previous measurements on halide salts of  $\text{Co}(\text{en})_3^+$  and  $\text{Cr}(\text{en})_3^{3+}$  in this region<sup>14,16</sup> confirms an increase in the population of the  $\lambda$ -ring conformation in going from the chloride to bromide to iodide salt. The  $\text{NH}$ -scissors modes for this complex were beyond the region of measurement in  $\text{DMSO}-d_6$ . However, our experimental measurements on the corresponding  $\text{Cr}(\text{III})$  complexes exhibit an intense negative VCD band for this mode at 1570  $\text{cm}^{-1}$  for  $\Lambda$ - $\text{Cr}(\text{en})_3\text{Cl}_3$  and a distinct intense (+/-) VCD couplet below 1600  $\text{cm}^{-1}$  for  $\Lambda$ - $\text{Cr}(\text{en})_3\text{I}_3$ ,<sup>16</sup> which correspond to the calculated intensity for  $\Lambda$ - $\text{Co}(\text{en})_3^{3+}$  conformers between 1700 and 1600  $\text{cm}^{-1}$ .

Our experimental and computational study of  $\text{Co}(\text{en})_3^{3+}$  agrees with previous X-ray,<sup>11,29</sup> NMR,<sup>19</sup> and electronic CD<sup>20,21</sup> studies, which have been used to identify the absolute configuration, assign solution conformations and study the effects of temperature and counterion concentration on the solution structure. However, these other methods cannot be used to identify the mode of chloride association with  $\text{Co}(\text{en})_3^{3+}$  in solution. We consider here possible association with the chloride ion lying along  $C_2$ -axes of the complex, bridging two  $\text{NH}$ -bonds from adjacent en rings, or lying along the  $C_3$ -axis, bridging three  $\text{NH}$ -bonds from adjacent en rings (see Figure 2). Both types of association stabilize the  $\delta$ -ring conformer. The VCD intensity calculations (Figure 10, Tables 1 and 2) show that the stretches of the  $\text{NH}$ -bonds associated with chloride ion on the  $C_2$ -axis generate an intense (+/-) VCD couplet, whereas stretches of the three  $\text{NH}$ -bonds associated with chloride lying on the  $C_3$ -axis generate a (-/+) VCD couplet. Comparison of these calculated spectra with the observed VCD for  $\text{Co}(\text{en})_3^{3+}$  in  $\text{DMSO}-d_6$  with a 10-fold excess of chloride ion (Figure 5, Table 2) clearly identifies the mode of chloride ion association in solution as along the  $C_3$ -axis. In addition, our calculations indicate that two chloride ions are associated with  $\text{Co}(\text{en})_3^{3+}$  under these conditions (association complex **1**), since the calculated spectra (not shown) for association of only one chloride ion along the  $C_3$ -axis predict that the positive VCD band assigned to free  $\text{NH}$ -stretch will have comparable intensity to the positive band for the associated  $\text{NH}$ -stretch, in contrast to the observed VCD spectrum and the calculated VCD spectrum for two chloride ions, for which the free  $\text{NH}$ -stretches (positive VCD  $\sim 3200 \text{ cm}^{-1}$ ) exhibit much weaker VCD. In the 1600–1100  $\text{cm}^{-1}$  region, excellent agreement in both frequency and intensity between observed spectra with excess chloride ion and calculated spectra for association complex **1** are found (Figure 6, Table 2). The calculated spectra for **2** (Figure 6) show a much poorer agreement with the observed spectra in the 1600–1100  $\text{cm}^{-1}$  region, both in frequency and intensity.

The DFT calculations produce an energy order for the four possible ring conformations and free energy values for conformational changes from the  $\delta\delta\delta$ -conformer that indicate an equilibrium in favor of the  $\lambda$ -ring conformation for the  $\Lambda$ -configuration of the free (gas-phase)  $\text{Co}(\text{en})_3^{3+}$  ion. Our solution

VCD spectra and previous NMR studies<sup>19</sup> are consistent with a predominance of the  $\delta$ -ring conformer for this configuration. This discrepancy suggests that interactions with the aqueous or DMSO solvent molecules or ion association with even the more weakly interacting halide counterions or sulfate ions (in the D<sub>2</sub>-SO<sub>4</sub> solutions) may stabilize the  $\delta$ -ring conformation.

VCD may be the only technique that can identify the location of chloride ion interaction with Co(en)<sub>3</sub><sup>3+</sup> in solution. Our calculations demonstrate that the local coupling of associated NH-stretches produces bisignate VCD couplets, the sense of which correlates with the location of the bound chloride. These VCD studies directly identify the preference for the  $\delta$ -ring conformation for the  $\Lambda$ -Co(en)<sub>3</sub><sup>3+</sup> in aqueous and DMSO solution, and the increase in population of the  $\delta$ -ring conformer with increasing chloride concentration. However, from our present studies, we cannot determine the fraction of rings in this conformation, since the VCD intensity for the case with all rings in the  $\delta$ -conformation is not yet known. The NMR determination of ring conformer population,<sup>19</sup> either with the use of coupling constants or chemical shifts, relies strongly on assumptions for the values for the ‘frozen’  $\lambda$  or  $\delta$  ring conformers for these systems, which rapidly interconvert on the NMR time scale. The VCD spectra are linear superpositions of the spectra of individual conformers, rather than averages, as is the case for NMR, but comparison of our calculations with the experimental data indicates that there are no spectral regions that contain unique VCD marker bands for individual ring conformations. The degree of agreement between experiment and calculation is not yet sufficient to use the ratio between NH- and CH-dominated VCD features for quantitative determination of the ring conformer populations.

This exploratory study reports the use of the LanL2DZ and 6-31G(d)[C, H, N]/Stuttgart ECP [Co] basis sets for VCD calculation, the first extensive application to a transition metal complex and the first calculation for a charged species with and without associated counterions. The effects of solvent are not included in the calculation. The qualitative agreement with experiment, that is, the agreement between calculated and experimental VCD intensity patterns, is excellent, including nearly all VCD signs and relative intensities, and the direction of frequency shift for NH modes with chloride association. Agreement of experimental and calculated magnitudes can partly be assessed from the  $\epsilon_{\max}$  and  $\Delta\epsilon_{\max}$  comparisons in Table 2, taking into account that a single spectral feature may result from several normal modes, and that bandwidths for experimental and calculated spectra may differ. The intensity magnitudes are similar for our calculations with the LanL2DZ and the 6-31G(d)[C, H, N]/Stuttgart ECP [Co] basis sets. In general, the calculated absorption intensities and VCD intensities for the chloride-associated ion (gas-phase values) are well within a factor of 2 of the observed data for the majority of the intense bands. This same pattern of agreement has been found for organic molecules calculated at the DFT/B3LYP/6-31G(d) level.

## Conclusions

Calculation of VCD spectra at the DFT/B3LYP/LanL2DZ basis set level for a closed-shell transition-metal complex, Co(en)<sub>3</sub><sup>3+</sup>, has provided confirmation of the absolute configuration assignment, identification of the dominant ring conformation in solution from VCD features characteristic of en-ring con-

formation, and a unique identification of the mode of association of chloride ion. Although the fractional ring conformer populations cannot be determined from this study, the calculations provide an understanding of the source of the variation of the observed VCD spectra with counterion concentration. This study provides a basis for application of VCD calculations to closed-shell transition metal complexes and a benchmark for extension to open-shell cases.

**Acknowledgment.** This work was partially supported by the National Computational Science Alliance and utilized the University of Kentucky HP N-4000 complex.

## References and Notes

- (1) Nafie, L. A.; Freedman, T. B. In *Circular Dichroism, Theory and Practice*; Nakanishi, K., Berova, N., Woody, W., Eds.; Wiley: New York, 2000; pp 97–131.
- (2) Nafie, L. A.; Freedman, T. B. *Enantiomer* **1998**, *3*, 283–297.
- (3) Nafie, L. A.; Freedman, T. B. In *Infrared and Raman Spectroscopy of Biological Materials*; Yan, B., Gremlish, H.-U., Eds.; Marcel Dekker: New York, 2001; pp 15–54.
- (4) Frisch, M. J.; Trucks, G. W.; Schlegel, H. B.; Scuseria, G. E.; Robb, M. A.; Cheeseman, J. R.; Zakrzewski, V. G.; Montgomery, J. A., Jr.; Stratmann, R. E.; Burant, J. C.; Dapprich, S.; Millam, J. M.; Daniels, A. D.; Kudin, K. N.; Strain, M. C.; Farkas, O.; Tomasi, J.; Barone, V.; Cossi, M.; Cammi, R.; Mennucci, B.; Pomelli, C.; Adamo, C.; Clifford, S.; Ochterski, J.; Petersson, G. A.; Ayala, P. Y.; Cui, Q.; Morokuma, K.; Malick, D. K.; Rabuck, A. D.; Raghavachari, K.; Foresman, J. B.; Cioslowski, J.; Ortiz, J. V.; Stefanov, B. B.; Liu, G.; Liashenko, A.; Piskorz, P.; Komaromi, I.; Gomperts, R.; Martin, R. L.; Fox, D. J.; Keith, T.; Al-Laham, M. A.; Peng, C. Y.; Nanayakkara, A.; Gonzalez, C.; Challacombe, M.; Gill, P. M. W.; Johnson, B.; Chen, W.; Wong, M. W.; Andres, J. L.; Gonzalez, C.; Head-Gordon, M.; Replogle, E. S.; Pople, J. A. *Gaussian 98*, version A.9; Gaussian, Inc.: Pittsburgh, PA, 1998.
- (5) Cheeseman, J. R.; Frisch, M. J.; Devlin, F. J.; Stephens, P. J. *Chem. Phys. Lett.* **1996**, *252*, 211–220.
- (6) Stephens, P. J.; Devlin, F. J. *Chirality* **2000**, *12*, 172–179.
- (7) Stephens, P. J.; Ashvar, C. S.; Devlin, F. J.; Cheeseman, J. R.; Frisch, M. J. *Mol. Phys.* **1996**, *89*, 579–594.
- (8) Devlin, F. J.; Stephens, P. J.; Cheeseman, J. R.; Frisch, M. J. *J. Phys. Chem. A* **1997**, *101*, 9912–9924.
- (9) Gigante, D. M. P.; Long, F.; Bodack, L. A.; Evans, J. M.; Kallmerten, J.; Nafie, L. A.; Freedman, T. B. *J. Phys. Chem. A* **1999**, *103*, 1523–1537.
- (10) He, Y.; Cao, X.; Nafie, L. A.; Freedman, T. B. *J. Am. Chem. Soc.* **2001**, *123*, 11320–11321.
- (11) Saito, Y.; Nakatsu, K.; Shiro, M.; Kuroya, H. *Acta Crystallogr.* **1955**, *8*, 729–730.
- (12) McCaffery, A. J.; Mason, S. F. *Mol. Phys.* **1963**, *6*, 359–371.
- (13) Stuart, B.; Peacock, R. D.; Alagna, L.; Prosperi, T.; Turchini, S.; Goulon, J.; Rogalev, A.; Goulon-Ginet, C. *J. Am. Chem. Soc.* **1999**, *121*, 10233–10234.
- (14) Young, D. A.; Freedman, T. B.; Lipp, E. D.; Nafie, L. A. *J. Am. Chem. Soc.* **1986**, *108*, 7255–7263.
- (15) Ernst, M. C.; Royer, D. J. *Inorg. Chem.* **1993**, *32*, 1226–1232.
- (16) Young, D. A. Ph.D. Dissertation, Syracuse University, 1986.
- (17) Corey, E. J.; Bailar, J. C., Jr. *J. Am. Chem. Soc.* **1959**, *81*, 2620–2629.
- (18) Piper, T. S.; Karipides, A. G. *J. Am. Chem. Soc.* **1964**, *86*, 5039–5040.
- (19) Hawkins, C. J.; Palmer, J. A. *Coord. Chem. Rev.* **1982**, *44*, 1–60.
- (20) Mason, S. F.; Norman, B. J. *J. Chem. Soc. A* **1966**, 307–312.
- (21) Smith, H. L.; Douglas, G. E. *Inorg. Chem.* **1966**, *5*, 784–788.
- (22) Lal, B. B.; Nafie, L. A. *Biopolymers* **1982**, *21*, 2161–2183.
- (23) Lipp, E. D.; Nafie, L. A. *Appl. Spectrosc.* **1984**, *38*, 20–25.
- (24) Nafie, L. A. *Appl. Spectrosc.* **2000**, *54*, 1634–1645.
- (25) Dunning, T. H., Jr.; Hay, P. J. In *Modern Theoretical Chemistry*; Schaefer, H. F., III, Ed.; Plenum: New York, 1976; Vol. 3, p 1.
- (26) Wadt, W. R.; Hay, P. J. *J. Chem. Phys.* **1985**, *82*, 284–298.
- (27) Stephens, P. J. *J. Phys. Chem.* **1985**, *89*, 748–752.
- (28) Dolg, M.; Wedig, U.; Stoll, H.; Preuss, H. *J. Chem. Phys.* **1987**, *86*, 866–872.
- (29) Nakatsu, K.; Saito, Y.; Kuroya, H. *Bull. Chem. Soc. Jpn.* **1956**, *29*, 428–434.